The mass function and distribution of velocity dispersions for UZC groups of galaxies

Armando Pisani

Astronomy Department, University of Trieste, via G.B. Tiepolo 11, I-34131 Trieste, Italy Istituto di Istruzione Statale Classica Dante Alighieri, Scientifica Duca degli Abruzzi e Magistrale S. Slataper, via XX settembre 11, I-34170 Gorizia, Italy

pisani@ts.astro.it

Massimo Ramella

INAF, Osservatorio Astronomico di Trieste via G. B. Tiepolo 11, I-34131 Trieste, Italy

ramella@ts.astro.it

and

Margaret J. Geller

Smithsonian Astrophysical Observatory 60, Garden Str., Cambridge, MA02138, U.S.A.

mjg@cfa.harvard.edu

ABSTRACT

We measure the distribution of velocity dispersions of groups of galaxies identified in the UZC catalog; we use the distribution to derive the group mass function. We introduce a new method which makes efficient use of the entire magnitude limited catalog. Our determination of $n(\geq \sigma_T)$ includes a significant contribution from low luminosity systems that would be missing in a volume limited sample. We start from a model for the probability density function of the total number of group members and reproduce the observed distribution. We take several effects like the local fluctuations in volume density, limited sampling and group selection into account. We estimate the relation between total number of members, total luminosity and true velocity dispersion. We can then reproduce not only the observed distribution of σ_v but also the distributions of the number of group members, the total groups luminosity, and virial mass. The best fit to the data in the true velocity dispersion range 100 km s⁻¹ $\leq \sigma_T \leq 750$ km s⁻¹ is a power law model with a slope $n(\geq \sigma_T) \propto \sigma_T^{-3.4^{+1.3}_{-1.6}}$ and a normalization $n(\sigma_T \geq 750 \text{ km s}^{-1}) = (1.27 \pm 0.21) \times 10^{-5} h^3 \text{ Mpc}^{-3}$ where σ_T is the true velocity dispersion of a group. The predictions of CDM models are consistent with the mass function we derive from this distribution of velocity dispersions.

Subject headings: galaxies: clusters: groups: general —- cosmology: observations —- cosmology: theory —- large scale structure of the universe

1. Introduction

Groups of galaxies contain approximately half of the galaxies within a magnitude limited redshift survey (see e. g. Ramella, Geller & Pisani 2002; Ramella, Pisani & Geller 1997; Trasarti-Battistoni 1998; Giuricin et al. 2000; Tucker et al. 2000; Adami & Mazure 2002; Merchán & Zandivarez 2002). In hierarchical structure formation theories, these abundant systems are the natural progenitors of the galaxy clusters. Thus measurement of the distribution of the physical parameters of groups provides part of the fundamental basis for understanding the large-scale structure of the universe (Zabludoff & Geller 1994; Nolthenius, Klypin & Primack 1994; Diaferio et al. 1999; Carlberg et al. 2000; Girardi & Giuricin 2000).

The velocity dispersion of a system of galaxies is an indicator of the depth of the potential associated with the system. Hence the distribution of velocity dispersions is the basis for the determination of the group mass function. Although the relation linking the velocity dispersion with the gravitational mass depends on the relative distribution of visible and dark mass and on the dynamical state of the galaxy system (Diaferio et al. 1993, but see also Xu, Fang & Wu 2000), the velocity dispersion itself is a physically interesting parameter. The data readily provide an estimate of the group velocity dispersion which is robust against the inclusion of faint members (Ramella, Geller & Huchra 1995; Ramella, Focardi & Geller 1996; Mahdavi et al. 1999). The small median number of group members introduces a large scatter in the observational estimate, σ_v , of the dispersion of a system relative to the true value, σ_T . This finite sampling effect also introduces distortion in the distribution of σ_v .

Several investigators have determined $n \geq \sigma_T$ for optical galaxy clusters (e. g. Bahcall et al. 2002; Reiprich & Böhringer 2002; Borgani et al. 1999; Girardi et al. 1998; Fadda et al. 1996; Mazure et al. 1996; Bahcall & Cen 1993; Biviano et al. 1993). In addition, there are also measurements of the cluster x-ray temperature function (Ikebe et al. 2002; Pierpaoli, Scott & White 2001; Blanchard et al. 2000; Henry 2000; Markevitch 1998; Henry & Arnaud 1991; Edge et al. 1990). On the theoretical side, large numerical simulations provide estimates of the predicted group/cluster mass function (e. g. Jenkins et al. 2001; Governato et al. 1999; Diaferio et al. 1999; Lacey & Cole 1994; Thomas et al. 1998). for a variety of cosmological models.

For galaxy groups with low luminosity and hence low velocity dispersion, some determinations of $n(\geq \sigma_T)$ rest on small samples of systems in volume limited catalogs (e.g. Zabludoff et al. 1993). Others contain residual biases resulting from the magnitude limit of the samples (e.g. Moore et al. 1993; Girardi & Giuricin 2000; Heinämäki et al. 2003). In principle, restriction to a volume limited catalog mitigates the problem of selection effects introduced by the apparent magnitude limit of the redshift survey (Zabludoff et al. 1993). However, low luminosity systems are virtually absent from volume limited catalogs.

The determination of $n(\geq \sigma_T)$ from magnitude limited samples requires correction for the selection function. The standard approach is to weight each group by the maximum volume where a group could still be recognized as a triplet. The weighting scheme assumes that throughout the mass range the catalog covers a fair sample of the universe. These determinations also assume that the mass-to-light ratio, M/L, is independent of velocity dispersion.

A reliable determination of the mass function of groups is particularly interesting because there are still significant discrepancies between theory and observations at the low-mass end of the distribution (Martínez et al. 2002; Heinämäki et al. 2003). Standard observational approaches to the determination of $n(\geq \sigma_T)$ are most uncertain at the low-mass end. For example Zabludoff et al. (1993) lack low-mass systems because of the absolute magnitude cut of their volume limited sample. For larger samples, the assumption of constant number of groups per unit volume is a potential problem. Even in these larger surveys, low mass systems probe a small volume where the distribution of systems is not homogeneous.

Here we introduce a method for constructing $n(\geq \sigma_T)$ from all of the groups identified in the magnitude limited UZC redshift survey. We improve the statistics of the $n(\geq \sigma_T)$ determination in the range $100 \text{ km s}^{-1} \leq \sigma_T \leq 750 \text{ km s}^{-1}$. We determine $n(\geq \sigma_T)$ in a homogeneous way throughout the entire range in σ_T . We account for the effects of limited sampling on the estimated velocity dispersion of each group and for local fluctuations in the number density of groups.

We demonstrate that in the UZC, the intrinsic relations among the luminosity, velocity dispersion and richness of groups are well-represented by power laws. By using these model relations we can satisfactorily account for the observed distributions of all the group parameters. These scaling relations for groups may be useful for evaluating the evolution of group properties in catalogs extracted from deeper surveys.

Section 3 discusses the group catalog. Section 4 outlines the main problems in estimating $n(\geq \sigma_T)$ and the basic method we apply. Section 5 discusses a power-law model for the relation between group richness and velocity dispersion. Section 6 describes the entire analysis method in detail and shows how we use the relation in Section 5. Section 7 contains the distribution of velocity dispersion and the group mass function. In Section 8 we discuss the scaling relations and demonstrate the broad consistency of the method we use. We summarize in Section 9.

2. The group catalog

We base our analysis on the UZC catalog (Falco et al. 1999) in the region defined by $-2.5^{\circ} \leq \delta_{1950} \leq 50^{\circ}$ and $8^{h} \leq \alpha_{1950} \leq 17^{h}$ in the North Galactic Cap and by $20^{h} \leq \alpha_{1950} \leq 4^{h}$ in the South Galactic Cap. In this region the completeness in redshift is 98%. We discard the region $-13^{\circ} \leq b \leq 13^{\circ}$ because of the greater Galactic absorption there (Padmanabhan, Tegmark & Hamilton 2001).

Ramella, Geller & Pisani (2002) describe the catalog of UZC groups and list the membership of all of the groups analyzed here. Ramella, Geller & Pisani (2002) identify the UZC groups with a friends-of-friends algorithm (FOFA) (Ramella, Pisani & Geller 1997; Huchra & Geller 1982). This algorithm is currently in wide use (Adami & Mazure 2002; Merchán & Zandivarez 2002; Girardi & Giuricin 2000; Tucker et al. 2000; Trasarti-Battistoni 1998) along with some applications of the dendogram analysis applied by Materne (1979) and by Tully (1987). The groups Ramella, Geller & Pisani (2002) identify are number density enhancements with $\delta \rho_N / \rho_N \geq 80$ in redshift space (α, δ, V).

The FOFA associates galaxies with a projected separation on the sky less than $D_0 = 0.25h^{-1}$ Mpc and a line-of-sight velocity difference less than $V_0 = 350$ km s⁻¹ at a reference fiducial velocity $v_F = 1000$ km s⁻¹. We scale the linking parameters $D_L = R(V) \times D_0$ and $V_L = R(V) \times V_0$ with a function R(V) according to the prescription of Huchra & Geller (1982). We assume that the UZC galaxy luminosity function (LF) is in the Schechter (1976) form and adopt $M_{\star} = -19.1$, $\alpha = -1.1$, and $\phi_{\star} = 0.04$ h^3 Mpc⁻³. We obtain these parameters by convolving the LF determined by Marzke et al. (1994) for a very similar sample with a Gaussian 0.3 magnitude error. These parameters improve those used by Ramella, Pisani & Geller (1997) to identify groups within the CfA2N survey. The differences between the Ramella, Pisani & Geller (1997) groups and the groups we identify now within the same region are negligible.

Within the UZC we identify 301 groups with at least 5 members and with mean velocities $500 \text{kms}^{-1} < V < 12000 \text{kms}^{-1}$. At the minimum group radial velocity $V_{min} = 500 \text{ km s}^{-1}$, the apparent magnitude limit of UZC, $m_{lim} = 15.5$, corresponds to an absolute magnitude $M_{lim} = m_{lim} - 25 - 5 \log(V_{min}/H_0) = -13.00 + 5 \log(h)$ and, with h = 1, to a luminosity $\log(L_{lim}/L_{\odot}) = 7.39$.

To eliminate 39 groups with very low intrinsic luminosity, we limit our analysis to groups with mean velocity $V \geq 3000$ km s⁻¹. We refer to the remaining $N_G = 262$ groups as the UZCGG sample. These groups have true velocity dispersions larger than ~ 2.5 times the errors in the individual redshift determinations. The lower limit in the true velocity dispersion of our 262 groups is comparable with the lower limit of the velocity dispersion of the x-ray emitting groups detected within UZCGG (Mahdavi et al. 1999).

In a group catalog selected from a redshift survey with a FOFA, some fraction of the groups are accidental superpositions. We have two measures of the fraction of true physical systems in the UZCGG. Ramella, Pisani & Geller (1997) use geometric simulations of the large-scale structure in the northern UZC region to demonstrate that 80% of the groups are probably physical systems. Diaferio et al. (1999) compare Λ CDM simulations with the northern portion of the UZC and conclude that the linking parameters we choose for group selection are in the optimal range for reproducing the catalog derived from n-body simulations. In that range the fraction of real groups is 70-80%. Mahdavi et al. (2000) cross-correlate a large portion of the UZCGG with the ROSAT All-Sky Survey (RASS). 61 groups in the Mahdavi et al. (1999) sample have associated extended x-ray emission. The presence of hot x-ray emitting gas bound in the group potential well is a confirmation of the physical reality of the system. Mahdavi et al. (2000) use the groups detected in the x-ray to show that a minimum fraction of 40% of the groups in the UZCGG subsample are similar x-ray emitting systems undetectable with the RASS; thus they set a lower limit of 40% on the fraction of real physical systems in the group catalog. At least 40% and probably 70-80% of the UZCGG systems are real and it is thus reasonable to use their properties to derive physical constraints on the nature of groups of galaxies.

3. The velocity dispersion distribution: the method

The group velocity dispersion is a fundamental quantity both for studying the internal dynamics of the group and for understanding the processes which produce these galaxy systems (Frenk et al. 1990; Moore et al. 1993; Weinberg & Cole 1993; Zabludoff et al. 1993; Crone & Geller 1995). It is therefore important to have a reliable estimate of the distribution of velocity dispersions for groups, the most common bound systems in the

universe.

Our goal is measurement of both the probability density of groups with a given velocity dispersion, $f(\sigma_T)$, and the space density of groups as a function of velocity dispersion, $n(\geq \sigma_T)$. One direct approach to the problem is analysis of a volume limited catalog of groups. This procedure significantly reduces the number of groups in the sample and, more importantly, it discards a large number of low luminosity systems largely with low velocity dispersions. For example, within the UZCGG there are 34 groups within the volume limited sample with velocity limit $V_{\star} = 8300$ km s⁻¹, and only 20 groups within $V_M = 12000$ km s⁻¹.

Undersampling the internal velocity field of each system also affects the determination of $n(\geq \sigma_T)$ for groups. The UZCGG groups have a median of 7 members: the estimate of their velocity dispersion σ_v (corrected for radial velocity uncertainty according to Danese, De Zotti & di Tullio 1980) has a large scatter around the true underlying velocity dispersion, σ_T . We use the unbiased estimator of Ledermann (1984) to compute σ_v . To illustrate the scatter, we use a Monte Carlo simulation to extract 1000 groups at random from a specified true distribution of σ_T . We simulate the "observed" group velocity dispersion σ_v under the assumption that peculiar velocities within the group are distributed according to a Gaussian with true dispersion σ_T . The distribution of mean radial velocity and richness of the simulated groups is the same as for the groups observed in the UZCGG sample. Figure 1 shows the relation between the true σ_T and the Monte Carlo sampled σ_v (the straight line represents equality of the two measures). The spread is quite large; it decreases at larger σ_v because the number of members observed is typically larger. For poorly sampled systems, the observed value of σ_v is a poor estimator of the true σ_T . In conclusion, the estimate of the distribution of the velocity dispersion is severely affected by several observational and sampling effects.

To avoid these difficulties we assume that the peculiar velocities of group member galaxies are gaussian-distributed. This assumption is warranted by our deeper sampling of groups with associated x-ray emission (Mahdavi et al. 1999). With an average of 35 galaxies per group, the velocity distributions are consistent with a Gaussian.

We simulate the observed value of σ_v by Monte Carlo-sampling of the Gaussian velocity field with dispersion σ_T . We use the data to demonstrate that there is a relation between σ_T and the absolute group richness N. We confirm the relation by examining a set of 43 more deeply sampled groups from Mahdavi et al. (1999) and Mahdavi & Geller (2001). We account for the selection effects introduced by: a) the apparent magnitude limit of the galaxy catalog, b) the distance dependent criterion of inclusion of a group in our analysis: $N_{mem} \geq N_{min} = 5$, and finally c) fluctuation in the space density of groups $\rho(V)$. We select groups according to the number of members. We therefore must estimate the probability density function, p(N), of the group absolute richness N, i.e. the total number of group members brighter than L_{lim} (or $M_{lim} = -13.00$). We use a power law model for p(N) and constrain both its slope and normalization. From p(N) we predict the number density of groups with more than N members.

By using the relation between group richness and velocity dispersion along with the estimate of p(N), we can compute both $f(\sigma_T)$ and $n(\geq \sigma_T)$. From these two distributions we can use Monte Carlo simulations to predict the observed distribution of σ_v . We can also predict the distribution of observed group luminosities, L_{mem} , provided that the luminosity function is universal.

The procedure includes the following steps:

- step 1: we estimate the relation between the number of group members (richness) N and the true velocity dispersion σ_T (Section 5)
- **step 2:** we choose a model for the probability density function of the group richness N: p(N) (Section 6)
- step 3 we estimate the group selection function by using p(N) (step 2) and then, by comparison with the data, we obtain the radial distribution of group density $\rho(V)$ (Section 6)
- step 4: by using the N vs. σ_T relation (step 1), the model for p(N) (step 2) and the estimate of $\rho(V)$ (step 3), we compute the cumulative distribution of the velocity dispersions $n(\geq \sigma_v)$ and compare it with the real data in order to assess the agreement with p(N)from step 2 (Section 7)
- step 5: by using the relations among richness, total luminosity, σ_T and the group mass, we compare the model distributions of all these quantities with the observations (Section 8).

The main advantages of this procedure are; a) we determine $n(\geq \sigma_T)$ for groups with L_T an order of magnitude fainter than for a volume limited catalog of groups identified within the same region b) we need not assume a constant space density of groups, and c) we use a sample of groups an order of magnitude larger than the the volume limited sample, and d) the mass function estimate does not require the assumption of constant M/L.

4. Group richness and velocity dispersion

Several investigators have explored the relationship between various measures of "richness" and the velocity dispersion of rich clusters of galaxies (Bahcall & Cen 1993): richer clusters tend to have larger velocity dispersions. Bahcall (1988), for example, fits a power-law relation between between the galaxy count within 0.25 h⁻¹ Mpc and the system velocity dispersion for 23 Abell clusters and a sample of groups (Turner & Gott 1976). More recently, Yee & Ellingson (2002) have shown that the richness of CNOC1 clusters of galaxies is well correlated with their main physical parameters as derived from both optical and x-ray observations. Here we use the UZCGG data along with a set of well-sampled x-ray emitting groups (Mahdavi et al. 1999; Mahdavi & Geller 2001) to examine the relationship between group richness and velocity dispersion.

We expect some relation between the total number of group members N and the true velocity dispersion, σ_T , because N and L_T are related through the luminosity function, L_T and mass are related for bound systems, and mass and velocity dispersion are also related (if light traces mass). We do not require the same M/L for groups at every velocity dispersion. As a simple approximation we choose a power-law model for the relation between n and σ_T :

$$N = N_0 \left(\frac{\sigma_T}{\sigma_0}\right)^a \tag{1}$$

where N_0 and σ_0 are scale factors and a is the exponent.

To estimate the parameters σ_0 and a, we fix an arbitrary normalization in number, $N_0 = 100$, and proceed in the following steps:

1. We select the i - th group from the sample at random. This group has $N_{mem}(i)$ members at a mean radial velocity V(i) and a total number of galaxies brighter than $M_{lim} = -13.0, N(i) = N_{mem}(i)/\nu(V(i)). \nu(V(i))$ is the fraction of galaxies detected in a group at mean radial velocity V(i):

$$\nu(V(i)) = \frac{\int_{L_{cut}(V(i))}^{+\infty} \phi(x) dx}{\int_{L_{lim}}^{+\infty} \phi(x) dx}$$
(2)

The luminosity $L_{cut}(V(i))$ corresponds to the UZC apparent magnitude limit at the radial velocity V(i) and $\phi(L)$ is the luminosity function.

The true velocity dispersion of the group is, according to our model,

$$\sigma_T(i) = \sigma_0 \left(\frac{N(i)}{N_0}\right)^{1/a} \tag{3}$$

- 2. We sample $N_{mem}(i)$ velocities from a Gaussian with standard deviation $\sigma_T(i)$ and compute the simulated velocity dispersion $\sigma_{sim,v}(i)$.
- 3. We repeat these steps until we obtain the desired number of simulated groups.
- 4. We perform a KS test between the simulated distribution of $\sigma_{sim,v}$ and the distribution of observed σ_v
- 5. We vary σ_0 and a in the interval $a \in [1; 3]$ and $\sigma_0(\text{ km s}^{-1}) \in [400; 600]$ in a 21×21 grid, and maximize the KS significance level.

We iterate the previous five steps ten times with 5000 groups in each iteration and compute the median of the KS-test significance S_{KS} of the comparison between the predicted and the observed distributions.

With this procedure applied to the UZCGG, we obtain $\sigma_0 = 510 \text{ km s}^{-1}$ and a = 1.8 with median $S_{KS}(\sigma_v) = 0.44$. The 99% confidence interval is (1.4; 2.1) for a and (460 km s⁻¹; 580 km s⁻¹) for σ_0 . The value of σ_0 is sensitive to the definition and scale of "richness."

Figure 2a shows the contours of constant $S_{KS}(\sigma_v)$ in the parameter space. The thick outermost isopleth is the 99% confidence level, the middle contour traces the 90% confidence level, and the inner thin contour traces the 50% confidence level. Note that the values of σ_0 are scaled for group richness estimated at $V \geq 3000 \text{ km s}^{-1}$ and hence for members brighter than -16.89. The corresponding value of the best fit σ_0 scaled to $V \geq 500 \text{ km s}^{-1}$ and $M_{lim} = -13.00 \text{ is } 230 \text{ km s}^{-1}$.

To test the model in equation eq. 1 further, we obtain σ_0 and a for a set of X-ray emitting groups kindly provided to us by A. Mahdavi (1999). Mahdavi et al. (2000) identified a set of groups with extended x-ray emission by cross-correlating a portion of the UZC with the ROSAT All-Sky Survey. The extended x-ray emission essentially guarantees the reality of the system. Mahdavi (1999) and Mahdavi (2003) obtained deeper redshift surveys of the groups and increased the typical membership to 30 galaxies. We use these enhanced data here to test the scaling relations derived for the UZC groups.

There are 43 groups in the Mahdavi sample with mean radial velocities $V \geq 5000 \text{ km s}^{-1}$ and galaxies brighter than $m \leq 16.5$. The average number of group members is 20 and hence the value of the velocity dispersion is estimated more reliably than for UZCGG. Moreover, the diffuse X-ray emission strongly reduces the false group identification problem. Figure 2b shows the KS-test confidence level contours for the X-ray sample. The best fit value for the slope *a* is 1.7. The 99% confidence intervals are (1.0, 2.7) for *a* and $(410 \text{ km s}^{-1}, 590 \text{ km s}^{-1})$ for σ_0 . Because of the different completeness limits and different cuts in mean radial velocity, the values of the σ_0 normalization in the two plots for X-ray and UZCGG differ by a factor 1.06. This offset improves the overlap of the contours in the σ_0 direction. Although the area covered by the contours is quite large, it is quite remarkable that X-ray groups yield values for a and σ_0 nearly coincident with the UZCGG sample.

Figure 3 shows N as a function of σ_v for the x-ray sample. The solid line is the result we obtained with the Monte Carlo procedure. The thin line is the bisector of the two fits obtained from a straightforward χ^2 fit to N vs σ_v and to σ_v vs N respectively. We find $\log(N) = 1.27^{+0.83}_{-0.42} \times \log(\sigma_v) - 1.47^{+1.14}_{-2.04}$ consistent with the Monte Carlo approach. The Monte Carlo yields a steeper slope because it weights less the rare groups with very low velocity dispersion which also depart from the $L_x - \sigma$ scaling relations (Mahdavi & Geller 2001).

Finally we note that our result agrees with the power law relation that Yee & Ellingson (2002) find between richness parameter, B_{cg} , and radial velocity dispersion, σ_1 , for CNOC1 clusters. Yee & Ellingson (2002) find $B_{cg} \propto \sigma_1^{1.8\pm0.2}$ within the range 600 km s⁻¹ $\leq \sigma_1 \leq$ 1300 km s⁻¹. The agreement is interesting also because there is only a marginal overlap between our high σ range and the low σ range of CNOC1 clusters.

5. The probability density function of groups

Here we investigate the probability density function of groups, p(N), for the UZCGG sample. Most (92%) of the groups have $N \leq N_r = 840$ (or $\sigma_T \leq \sigma_r = 750 \text{ km s}^{-1}$). Sparse sampling of the richest systems (clusters) limits the range over which we can reliably estimate p(N) to 20 < N < 840. In our determination of p(N), we include all groups. Groups with with $N \geq N_r$ are visible (i.e. $N_{obs} \geq 5$) throughout the whole sample volume. These groups have marginal weight in the determination of the slope of p(N) but they are important for the normalization of $n(\geq \sigma_T)$.

We assume a power-law model for p(N):

$$p(N) = A \left(\frac{N}{N_{norm}}\right)^{-\gamma} \tag{4}$$

where N_{norm} is a scale factor and A is a normalization constant.

Here we set $N_{norm} = N_{min}$, with $N_{min} = 5$ (see the previous section). We note that the choice of N_{norm} is arbitrary because the power-law is scale free.

The Press & Schechter (1974) formalism, PS hereafter, provides a basis for this assump-

tion. Valageas & Schaeffer (1997) argue that in the low mass range occupied by poor galaxy systems the probability density function p(N) is well described by a power law. Recently, Jenkins et al. (2001) use numerical simulations to obtain similar results. We make the argument appropriate for our data here.

The PS model describes the mass function as:

$$n_{PS}(M)dM = K\left(\frac{M}{M_{\star}}\right)^{\alpha} \exp\left(-\left(\frac{M}{M_{\star}}\right)^{\beta}\right) d\left(\frac{M}{M_{\star}}\right).$$
(5)

where K is a normalization factor, M_{\star} is a scale factor and the exponents α and β are linked to the spectral index, n_{eff} , of primordial mass fluctuations: $\alpha = n_{eff}/6 - 3/2$ and $\beta = 1 + n_{eff}/3$. If we suppose that the group mass M is a power law function of the group number of galaxies N,

$$M \propto N^k \tag{6}$$

we can rewrite the mass function in terms of N:

$$n_{PS}(N)dN = K'\left(\frac{N}{N_{\star}}\right)^{\alpha k+k-1} \exp\left(-\left(\frac{N}{N_{\star}}\right)^{\beta k}\right) d\left(\frac{N}{N_{\star}}\right)$$
(7)

The local slope of the PS model is:

$$\gamma = \frac{d}{d\ln(x)} \ln n_{PS}(x) \tag{8}$$

where $x = N/N_{\star}$. In other words:

$$\gamma = \beta k x^{\beta k} - \alpha k - k + 1 \tag{9}$$

The slope γ depends on x and hence on N, but for the range of interest here ($20 \leq N \leq 840$), γ goes from 2.2 to 3.3. This range is in good agreement with the 90% confidence interval in our fit, namely (2.7, 3.2) (see section 7). By taking N as the average value $\langle N \rangle$ of the N estimated for the observed groups, we can conclude that Equation 9 links the two parameters n_{eff} and N_{\star} that characterize the PS model. Given a value of n_{eff} we should obtain a "best fit" N_{\star} :

$$N_{\star} = < N > \left(\frac{\beta k}{\gamma + \alpha k + k - 1}\right)^{1/(\beta k)} \tag{10}$$

is shown in Figure 4.

Over the range covered by our data, the Press-Schechter model is well-approximated by a simple power law model for the mass and N functions.

We next evaluate γ in Eq. 4 from the observed group catalog. We start by estimating the probability of finding a group at mean velocity V with at least five observed members, $N_{mem} \geq N_{min} = 5$. We call this function the group selection function, $\Sigma(V)$.

The probability that a group has at least N total members is:

$$S(N) = \int_{N}^{+\infty} p(x)dx \tag{11}$$

with S(N) normalized so that $S(N_{norm} = N_{min} = 5) = 1$.

Consequently, the group selection function $\Sigma(V)$ is:

$$\Sigma(V) = S\left(\frac{N_{min}}{\nu(V)}\right) \tag{12}$$

Clearly, $\Sigma(V)$ depends on both $\phi(L)$ and p(N).

From the group selection function, we can compute the distributions of V and N_{mem} from the model for p(N). The distribution of group radial velocities is:

$$C(V) = \int_{V_m}^{V} \Delta \Omega v^2 \rho(v) \Sigma(v) dv$$
(13)

where $V_m = 3000 \text{ km s}^{-1}$, $\Delta \Omega = 3.16 \text{ sr}$ is the solid angle of UZCGG, and $\rho(V)$ is the density of groups as a function of their mean radial velocity. The distribution of observed members is:

$$Q(N_{mem}) = \int_{V_m}^{V_M} \Delta \Omega v^2 \rho(v) S\left(\frac{N_{mem}}{\nu(v)}\right) dv$$
(14)

with $V_M = 12000 \text{ km s}^{-1}$, the redshift limit of the group catalog.

We compare the simulated C(V) and $Q(N_{mem})$ with the observed distributions of the same quantities. To make the comparison we must solve a system of two equations in the two functions p(N) and $\rho(V)$. We have an assumed form for p(N). To estimate $\rho(V)$ we invert the equation for C(V) (Eq. 13). We approximate $\rho(V)$ with a sequence of N_{shell} radial velocity shells, each with constant density, i.e.:

$$\rho(V) = \rho_i \ if \ V_{i-1} < V \le V_i \tag{15}$$

with $i = 1, \ldots, N_{shell}$. If there are δN_i observed groups within the i - th shell, ρ_i is:

$$\rho_i = \frac{\delta N_i}{\Delta \Omega \int_{V_{i-1}}^{V_i} v^2 \Sigma(v) dv}$$
(16)

We choose the limits of the shells, V_i , so that all shells contain the same number of groups. We start with $N_{shell} = 1$ and perform a KS-test to estimate the significance $S_{KS}(V)$ of the agreement between the model prediction C(V) and the observed distribution of V. We increase N_{shell} until $S_{KS}(V) \ge 0.5$.

We have thus derived a reasonable approximation to $\rho(V)$ and we next use it in eq. 14 to compute $Q(N_{mem})$. We use a KS-test to evaluate the agreement between $Q(N_{mem})$ and the observed distribution of N_{mem} . If the agreement is satisfactory, we conclude that we have a satisfactory slope for p(N). If, on the contrary, the distributions are inconsistent, we repeat the whole procedure with a different slope for p(N). Once we determine $\rho(V)$ and p(N), we can compute the total abundance of seen and unseen groups richer than a fixed threshold within the UZCGG volume, i.e. the group multiplicity function $\mu(\geq N)$.

The total number \mathcal{N}_G of groups within UZCGG is:

$$\mathcal{N}_G = \Delta \Omega \int_{V_{min}}^{V_{max}} v^2 \rho(v) dv \tag{17}$$

and the group average density is:

$$\bar{\rho} = \frac{\mathcal{N}_G}{\mathcal{V}} \tag{18}$$

where $\mathcal{V} = 1.79 \times 10^6 \ h^{-3} \ \text{Mpc}^3$ is the UZCGG volume. Under the assumption that p(N) does not depend on position within the UZCGG volume, the multiplicity function is:

$$\mu(\geq N) = \bar{\rho} \int_{N}^{+\infty} p(x) dx \tag{19}$$

For groups with N large enough to be observable throughout the UZCGG volume, we can compare our model prediction $\mu(N)$ directly with the observations. We call these groups **robust** and use them in order to normalize the function $\mu(\geq N)$.

To go from p(N) and $\mu(\geq N)$ to $n(\geq \sigma_T)$ we use the relation between N and σ_T (equation 1). The data constrain the power-law slope a and the normalization σ_0 . The relations we need are:

$$f(\sigma_T) = p(N) \frac{dN}{d\sigma_T}$$
(20)

and

$$n(\geq \sigma_T) = \bar{\rho} \int_{\sigma_T}^{+\infty} f(x) dx \tag{21}$$

We can compute $n(\geq \sigma_T)$ by inserting equation 4 into equation 20.

Because σ_T is related to N as in the eq. 1, we can write

$$f(\sigma_T) = \left(\frac{\sigma_T}{\sigma_{norm}}\right)^{-\gamma_s} \tag{22}$$

with $\gamma_s = \gamma a - a + 1$ and σ_{norm} is a normalization scale.

To estimate the value of the exponent γ we compare the observations with the predictions of the p(N) model obtained by inserting eq. 4 for p(N) into eq.s 13 and 14. The best fit value is $\gamma = 2.9$ with a 90% confidence level interval (2.7; 3.2). Figure 5 shows the KS significance level S_{KS} vs γ . The curve is very well behaved. This fit requires $N_{shell} = 7$ homogeneous density shells (see eq. 15). We show the density function $\rho(V)$ for the 7 shells in Figure 6; the density rises steeply at large V (last two shells). If we remove these shells from the analysis, the results do not change significantly. With $\gamma = 2.9$ our model is consistent with both the observed cumulative distribution of N_{mem} and the radial velocity distribution with significance levels of $S_{KS}(N_{mem}) = 0.73$ and $S_{ks}(V) = 0.62$ respectively.

6. The distribution of velocity dispersions and the group mass function

To compare with models we derive the velocity dispersion distribution and the mass function. Diaferio et al. (1999) make an exhaustive comparison of groups catalogs derived from the τ CDM and Λ CDM simulations by Kauffmann et al. (1999) with catalogs derived from CfA2N, subset of the UZC. They use the same FOFA we employ and vary the linking parameters over a wide range. They also test the sensitivity of their results to variations in the luminosity function and to the presence of structures like the Great Wall. They demonstrate that for the linking parameters we use here, the catalog derived from the data agree reasonably well with the catalogs derived from Λ CDM provided that the luminosity density is the same in both cases. They show that the normalization of the distribution of velocity dispersions (and of the mass function) is much more sensitive to the luminosity density than to variation in the linking parameters in the group finding algorithm over a reasonable range. They emphasize that the Great Wall plays an important role in biasing the distribution of velocity dispersions and the mass function toward higher values relative to the simulations. We see a similar effect and comment further below.

In the previous section we obtain the best fit value $\gamma = 2.9$ (90% c.l. (2.7;3.2)) for the exponent of the power-law probability density function of groups, p(N). We conclude that, at high confidence level, the density of galaxy systems with true velocity dispersion larger than σ_T is:

$$n(\geq \sigma_T) = (1.27 \pm 0.21) \times 10^{-5} h^3 \,\mathrm{Mpc}^{-3} \left(\frac{\sigma_T}{750 \,\mathrm{km\,s}^{-1}}\right)^{-3.4^{+1.3}_{-1.6}}$$
(23)

This distribution applies over the range $100 \text{ km s}^{-1} \leq \sigma \leq 750 \text{ km s}^{-1}$. The volume covered by the group catalog is too small to include many rich clusters. Within the UZCGG there are 20 (robust) groups visible throughout the entire UZCGG volume. These groups have $N \geq N_r = 840$ corresponding to a true velocity dispersion $\sigma_r = 750 \text{ km s}^{-1}$ (see eq. 1), the actual upper limit of the range of N (and σ_T) over which we determine p(N). For the high- σ_T systems our analysis does not provide an estimate of the slope of p(N), but it does provides an estimate of the abundance of these systems: $\mu(N_r) = 1.27 \times 10^{-5} h^3 \text{ Mpc}^{-3}$. We compute the Poisson uncertainty in $\mu_{obs}(N_r)$ in the number of observed groups N_G : $\delta \mu_{obs}(N_r) = 0.25 \times 10^{-5} h^3 \text{ Mpc}^{-3}$ and conclude that our prediction with the observed value $\mu_{obs}(N_r)$ to within $0.68 \times \delta \mu_{obs}(N_r)$.

We also compare our determination of the abundance of massive systems with previous surveys. Direct comparison is possible with Mazure et al. (1996); Fadda et al. (1996); Zabludoff et al. (1993). These authors give $n(\geq \sigma_T)$ for clusters. Their system abundances at $\sigma = 750 \text{ km s}^{-1}$, are 0.2, 0.6, and $0.6 \times 10^{-5} h^3 \text{Mpc}^{-3}$ respectively. Our system abundance is $n(\geq 750) = 1.3 \times 10^{-5} h^3 \text{Mpc}^{-3}$. Internal errors are of the order of few tenths in units of 10^{-5} . These errors reflect the size of the samples and may be less important than the systematic errors introduced by various selection effects. To examine the discrepancy between our estimate of $n(\geq 750)$ and previous ones, we summarize the characteristics of the different samples.

The ENACS clusters (Mazure et al. 1996) lead to the lowest abundance of systems. ENACS is a sample of Abell clusters selected according to a richness criterion. Abell clusters are an incomplete set of systems (see e. g. Gal et al. 2003, DPOSS2). More importantly, selection according to Abell richness produces a biased sample of velocity dispersions. Mazure et al. (1996) are aware of this problem and discuss it in detail. The velocity dispersions of clusters selected according to richness are biased high because σ increases with richness and because there is a broad scatter around the mean relation. Mazure et al. (1996) use reasonable arguments to identify a threshold, $\sigma = 800 \text{ km s}^{-1}$, above which their cluster catalog is unbiased. In the end, however, unbiasedness remains an assumption. The abundance derived by Fadda et al. (1996) is a factor of three larger than Mazure et al. (1996). Fadda et al. (1996) add poorer systems to the ENACS sample. In order to have a σ distribution that takes into account poor systems, Fadda et al. (1996) scale their richness distribution to mimic that of the Edinburgh-Durham Cluster Catalog (EDCC: Lumsden et. al. 1992). EDCC is probably a more complete catalog than Abell-ACO, especially at the low richness end. Fadda et al. (1996) perform 10,000 random samplings of the velocity dispersions of their systems, constraining the richness distribution of the bootstrapped sample to be the same as that of EDCC systems. This analysis leads to the same cluster abundance as Zabludoff et al. (1993), who use a combined sample of Abell clusters and the thirty densest groups selected within the first two slices of the CfA2N redshift survey (Ramella, Geller & Huchra 1989).

We select systems in redshift space from a complete magnitude limited galaxy catalog similar to but more extensive than the one used by Zabludoff et al. (1993). In contrast with Zabludoff et al. (1993), we include relatively poor systems that would enter neither a volume limited sample nor a 2D-selected sample. In fact, because of the large scatter around the mean relation between σ and richness, several of these relatively poor systems have velocity dispersions $\sigma \geq 750$). It is therefore not surprising that we find a higher abundance of systems above this threshold.

Other optical and x-ray studies have returned lower system abundances. Bahcall & Cen (1993), for example, argue that the abundance of clusters with velocity dispersion larger than 750 km s⁻¹ is $0.2 \times 10^{-5} h^3 \text{Mpc}^{-3}$, much lower than our estimate. They use a richness limited sample of Abell clusters and obtain a scaling relation $M \propto \sigma^2$ significantly different from ours (see Table 1).

The abundance of clusters can also be estimated from x-ray selected samples. The comparison of our abundance of systems with that of x-ray clusters requires a relation between x-ray temperature and velocity dispersion and/or mass. The scatter around this relation is the source of considerable uncertainty. Reiprich & Böhringer (2002) have carefully analyzed the abundance of clusters derived from x-ray data. In the range $2.55 \times 10^{14} M_{\odot} \leq M \leq$ $4.4 \times 10^{14} M_{\odot}$ the cluster abundance is $1.4 \times 10^{-6} h^3 \text{ Mpc}^{-3} \leq n (\geq M) \leq 7.0 \times 10^{-6} h^3 \text{ Mpc}^{-3}$. They conclude that the abundance of x-ray clusters is generally lower by a factor of 1.2 - 6.2than that of optically selected clusters (Girardi et al. 1998). The origin of the discrepancy may be either intrinsic –optical and X-ray clusters may belong to different populations– or may result from observational biases affecting the mass estimates.

We may overestimate $n \geq 750$ somewhat because of (1) projection effects in redshift space, (2) large-scale inhomogeneities in the galaxy distribution, and (3) systematic errors in catalog magnitude limits. N-body and geometrical simulations indicate that 20% of the 5-member groups we study are accidental superpositions. X-ray observations (Mahdavi et al. 2000) indicate that at least 40% of the groups we study are true physical systems. It is difficult to correct our $n(\geq \sigma_T)$ for the presence of false groups since we know their abundance nor their velocity dispersion distribution. Whatever the correction, our $n(\geq 750)$ would decrease to come into closer agreement with the estimates of Zabludoff et al. (1993) and Fadda et al. (1996).

Another possible effect driving our abundance toward a high value is the possible overluminosity of the UZC catalog from which we derive our group catalog (Ramella, Geller & Pisani 2002). The Zwicky magnitude system may be deeper than implied by its formal magnitude limit. In this case, we detect more systems than we should within the surveyed volume of the Universe. The density of systems could be too high by as much as a factor two. Correction for this effect would bring our estimate of massive systems into close agreement with Fadda et al. (1996) and with Zabludoff et al. (1993).

Finally, it is possible that the region of the UZC is overdense. The abundance of groups is proportional to the galaxy density across many different surveys (see e. g. Ramella et al. 1999). Variations in the density on the scale of the UZC may be as large as a factor of 2, but not more. Further, Diaferio et al. (1999) emphasize that the presence of the Great Wall in the northern portion of the UZC biases the groups sample toward higher luminosity and velocity dispersion relative to a typical regions extracted from a Λ CDM simulation. The groups in the Great Wall are at a larger velocity (~ 8000 km s⁻¹) than the median groups redshift (~ 6000 km s⁻¹) in a simulated region. These effects may contribute substantially to the high normalization of the mass function we derive.

We next review estimates of the mass function of groups. Girardi & Giuricin (2000) measure the mass function of a sample of groups. A direct comparison between their masses and ours is not straightforward because their masses are obtained in a model dependent way. Taken at face value (see Fig. 9), their mass function is not significantly different from ours. Our estimate, however, extends toward lower masses by almost an order of magnitude.

Heinämäki et al. (2003) estimate the mass function of the Las Campanas Redshift Survey groups (Tucker et al. 2000). The amplitude of their mass function is very low (less than $0.1 \times 10^{-5} h^3 \text{Mpc}^{-3}$ for masses roughly corresponding to $\sigma = 750 \text{ km s}^{-1}$. Heinämäki et al. (2003) compare their mass function with the results of Girardi & Giuricin (2000) and with N-body simulations (see Fig.7 in Heinämäki et al. 2003). The comparison demonstrates the generally low abundance of systems and the marked flattening of the LCRS group mass function with respect to the simulated mass function at the low mass end. We obtain a similar flattening when we do not take the large-scale variation of group number density into account. Low mass groups are undersampled and a V/V_{max} weighting scheme does not fully recover them.

Martínez et al. (2002) analyze a 2dF sample of groups (Merchán & Zandivarez 2002). In this case, as the authors recognize, the flattening of the mass function at low mass results from the low number cut-off imposed on their group identification procedure. Martínez et al. (2002) compare their mass function with N-body simulations (Jenkins et al. 2001) and claim good agreement. Because their best fit agrees with the Λ CDM model, their result is marginally consistent (~ 95%) with ours.

In Figure 7 we plot $n(\geq \sigma_T)$ and its 95% confidence level corridor. There we also plot the velocity dispersion distribution obtained by Zabludoff et al. (1993) (long dash). As expected, the Zabludoff et al. (1993) volume limited sample does not include low velocity dispersions systems.

By using the relations between richness and mass (see Eq. 6 and Table 1), and between richness and velocity dispersion (eq. 1) we can convert $n \geq \sigma_T$ into an estimate of the mass function. We compare this determination with the simulations of Jenkins et al. (2001, Virgo Consortium) who derive predictions for the mass function of systems of galaxies over our observed mass range. Because the theoretical mass functions predicted by Jenkins et al. (2001) apply to masses of critical overdensities, $(\delta \rho_c / \rho)_m$, we scale their masses to match our group number overdensity threshold $(\delta \rho_c / \rho)_N = 80$. We perform the scaling as in Borgani et al. (1999) for both of the cosmological models in Jenkins et al. (2001), Λ CDM $(\Omega_m = 0.3, \Omega_{\Lambda} = 0.7, \sigma_8 = 0.9)$ and τ CDM with $(\Omega_m = 1, \Omega_{\Lambda} = 0, \sigma_8 = 0.6)$.

Figure 8 compares our power law determination of the mass function with the theoretical results of Jenkins et al. (2001). We plot the cumulative mass function $n(\geq M)$ versus the mass M. The solid line represents our power law estimate, the dotted lines are 95% confidence levels. The τ CDM mass functions lies within the 95% confidence level over the mass range. The mass function predicted by the Λ CDM cosmology is only marginally consistent with our observations. If we correct the mass function normalization for the presence of unphysical groups, the agreement with the Λ CDM model improves.

The agreement of our observations with the theoretical mass function is remarkable. The use of our weighting procedure is critical in obtaining this result. In fact, if we use the standard approach and weight each group by its maximum accessible volume, V/V_{max} , we obtain the thin long-dashed curve in Figure 9. This curve shows the characteristic bending to a shallower slope at low masses. As discussed above, this shallower slope appears in other observed mass functions (e.g.: Martínez et al. 2002; Girardi & Giuricin 2000). Our procedure extends the determination of the mass function to masses almost one order of

magnitude lower than previous estimates.

7. Consistency tests and scaling relations

The mass function we derive depends on the estimate of the two functions $\rho(V)$ and p(N). We now show that, starting from these two functions, we can reproduce the observed distributions of all the main physical parameters of groups, i.e. V, N_{mem} , L_{mem} , σ_v , and virial mass, M_{vir} .

We proceed in the following way: we randomly sample $\rho(V)$ and generate a group with N members brighter than L_{lim} . We estimate the number of visible members, N_{mem} , as $N_{mem} = N \cdot \nu(V)$, according to 2. We discard the group if N_{mem} is less than 5. If we have at least 5 members, we estimate L_{mem} by randomly sampling the Schechter (1976) LF N_{mem} times. Finally, we estimate σ_v by randomly sampling a gaussian with dispersion σ_T , where we compute σ_T from the best fit model equation 1. We could estimate the virial mass by using the true velocity dispersion $\sigma_T : M_T = 3\sigma_T^2 R_{vir}/G$. However, in the usual analysis of an observed group catalog, the value of σ_T is not available and the standard estimate of the virial mass is $M_{vir} = 3\sigma_v^2 R_{vir}/G$. We simulate the observationally derived value of M_{vir} in the following way. We compute the scaling relations between, for example, N and M_T by using the bisector of the two straight lines we obtain first by least squares of $\log(M_T)$ versus $\log(N)$ and second by least squares of $\log(N)$ versus $\log(M_T)$. We compute the simulated value of M_{vir} as $M_{vir} = M_T(\sigma_v/\sigma_T)^2$.

We stop the previous Monte Carlo simulations when we reach a total of 1000 observable groups. We compare the simulated to the observed distributions and compute the significance of the agreement between the two distributions with a KS-test. We repeat the whole procedure 10 times and take the median KS significance level as a measure of the agreement between the distributions.

We obtain the following median values of S_{KS} : 0.43, 0.76, 0.29, 0.15, and 0.34 for V, N_{mem} , L_{mem} , σ_v , and M_{vir} respectively. Figure 10 shows the distributions of the physical parameters of 1000 simulated groups (thin line) together with the corresponding distributions for the observed groups (thick line). The agreement between the observations and the predictions of the simulations indicates that our model is a satisfactory representation of the data.

To test the sensitivity of the exponent γ in the p(N) model, to the parameters of the N vs. σ_T law, we use the most extreme values of the parameters a and N_0 in Eq. 1 within the 99% confidence level contour (see Figure 2a). With these parameter values it is impossible to

recover both the observed distributions of the group members N_{mem} and velocity dispersion σ_v .

Table 1 lists the scaling relations we obtain. We determine the scaling relations as the angular coefficient and intercept of the bisector of the two straight line fits X versus Y and Y versus X, with X and Y any two related quantities in Table 1. We use the results of the two fits to characterize the uncertainty in the scaling relations.

We actually use the relation between mass, M, and richness, N, (Eq. 6) or, equivalently, between M and the velocity dispersion, σ , to translate $n(\geq \sigma_T)$ into a mass function, $n(\geq M)$. We also use this relation to recover the observed distribution of the virial mass M_{vir} .

Once we establish the relation between M and N, we also have a relation between M and luminosity, L. As expected, the slope of $\log(M)$ vs. $\log(N)$ and the slope of $\log(M)$ vs. $\log(L)$ are indistinguishable. Girardi et al. (2002) analyze the relation between M and L for a different sample of groups and clusters. They obtain $M \propto L^{1.34\pm0.03}$, within about one sigma of our relation.

N-body simulations and semianalytic modeling of galaxy formation performed by Kauffmann et al. (1999) and Benson et al. (2000) gave a reliable prediction of the M/L ratio for galaxy systems and also provide an estimate of the dependence of mass-to-light ratio, M/L, on L (or M). It is generally found that the ML ratio increases from poor to rich systems, and eventually flattens on large scales.

Yee & Ellingson (2002) measure the relation between mass and richness (B_{cg}) within the CNOC1 sample of clusters of galaxies. These authors find $M \propto B_{cg}^{1.64\pm0.28}$, in very good agreement with our result. Because the intercept of this relation depends on the magnitude completeness limit, we can compare only slopes and not intercepts.

As a consistency check, we also compute the relation between $\log(L_T)$ and $\log(\sigma_T)$. Reassuringly, the slope of this scaling law is the same as our best fit of the power law model in Eq. 1, N vs. σ_T .

Finally, for the sake of completeness, in Table 1 we list the relations between $\log(M)$ vs. $\log(\sigma_T)$, $\log(N)$ vs. $\log(R_{vir})$ and $\log(\sigma_T)$ vs. $\log(R_{vir})$. Yee & Ellingson (2002) fit the scaling between the virial radius and richness and find $B_{cg} \propto R^{2.1\pm0.7}$, in very good agreement with our result. Our scaling relations significantly extend the data range spanned by cluster analyses. These scaling relations are remarkably consistent with those derived for clusters.

We also explore different forms for p(N). For example, we consider a p(N) that gives an exponential law for $f(\sigma_T)$, i.e. the law used by Zabludoff et al. (1993). This form for p(N) fails to reproduce the space density of robust groups $\mu_{obs}(\geq N_r)$ and leads to a discordant

distribution of L_{mem} . Another model we test is the PS model. The problem with this model (Equation 7) is that it has two free parameters, n_{eff} and N_{\star} : our procedure can constrain only one parameter (see section 6). However, we can test the relation between n_{eff} and N_{\star} if p(N) can be approximated by a power-law (see Equation 10). We compare the PS model for p(N) with our data using a KS test. In Figure 4 we plot the 10%, 50%, and 99% confidence level contours in the n_{eff} — N_{\star} plane. In the same plane we also plot N_{\star} as a function of n_{eff} according to Equation 10 where we assume $\langle N \rangle = 300$, close to the average value for our sample. For γ we use our best fit value, $\gamma = 2.9$. Figure 4 clearly shows good agreement between the power-law approximation and the PS model (note that the rejection region is external to the outermost contour (c.l. 99%)).

Sato et al. (2000) determine $n_{eff} = -1.2 \pm 0.3$ for masses in the range $10^{12} - -10^{15} M_{\odot}$ based on the analysis of an ASCA x-ray cluster sample. Zandivarez, Abadi & Lambas (2001) find similar results for these scales. If we use the value $n_{eff} = -1.2$ in Equation 7, we obtain a PS model with $N_{\star} \simeq 280$ corresponding to $M_{\star} = 1.6 \times 10^{14} h^{-1} M_{\odot}$ (95% confidence interval goes from $6.5 \times 10^{13} h^{-1} M_{\odot}$ to $3.6 \times 10^{14} h^{-1} M_{\odot}$). This value of M_{\star} is in reasonable agreement with the determinations of Bahcall & Cen (1993), namely $M_{\star} = (1.8 \pm 0.3) \times 10^{14} h^{-1} M_{\odot}$ and Girardi et al. (1998): $2.6^{+0.8}_{-0.6} \times 10^{14} h^{-1} M_{\odot}$. This result indicates that our analysis of low-mass systems of galaxies leads to an estimate of the mass function parameters consistent with the results determined in the higher mass range of galaxy clusters.

8. Summary

We measure the probability density function for the velocity dispersion of groups in the UZC galaxy catalog. Our method a) does not require that the group spatial density is constant, b) predicts the observed distributions of all the fundamental quantities of groups, i.e radial velocity, number of members, luminosity, velocity dispersion, and virial mass, and c) includes low luminosity systems that would be neglected with the usual analysis of a volume limited sample. The best fit for the slope of $n(\geq \sigma_T)$ is -3.4 (-2.6; -4.7) over the range 100 km s⁻¹ $\leq \sigma \leq 750$ km s⁻¹. Over this range, the Press-Schechter model is wellapproximated by a simple power law model. Our model predictions agree quite well with the predictions of Jenkins et al. (2001) for the CDM models.

Our weighting procedure is critical in the mass function determination. If we use the standard approach and weight each group by its maximum accessible volume, V/V_{max} , we obtain the characteristic bending of the mass function to a shallower slope at low masses. This shallower slope appears in other observed mass functions (e. g. Martínez et al. 2002;

Girardi & Giuricin 2000). Our procedure extends the determination of the mass function to masses almost one order of magnitude lower than previous estimates.

For massive systems, the density of groups with true velocity dispersion larger than 750 km s⁻¹ is $(1.27 \pm 0.21) \times 10^{-5} h^3$ Mpc⁻³. Our determination is larger by a factor of two than previous determinations. We examine this discrepancy and identify several possible sources for this discrepancy: a) incompleteness of cluster catalogs used in previous works, b) presence of false groups in our catalog produced by projection effects in redshift-space, c) systematic errors of the Zwicky magnitude system (may be deeper than its nominal magnitude limit would imply), d) real overdensity of the region of the UZC. Corrections for any of these effects would bring the abundance determinations into closer agreement.

The mass function we derive depends on the estimate of the two functions $\rho(V)$ and p(N). Starting from these two functions, we reproduce the observed distributions of all the main physical parameters of groups, i.e. V, N_{mem} , L_{mem} , σ_v , and virial mass, M_{vir} . We also obtain scaling relations between these physical parameters. Our scaling relations significantly extend the data range spanned by cluster analyses and are remarkably consistent with those derived for clusters.

9. Acknowledgments

We benefited from extensive discussions with Antonaldo Diaferio about the comparison between observed and simulated group catalogs. We thank Andisheh Mahdavi for providing us with the data of x-ray emitting groups. We also thank Adrian Jenkins for his help with the CDM mass functions. We thank the anonymous referee for helpful suggestions. This work was partially supported by the Italian Space Agency (ASI) and by Italian Ministry of Education, University and Research (MIUR grant COFIN 2001028932).

REFERENCES

Adami, C., & Mazure, A. 2002, A&A, 381, 420

- Bahcall N., A. 1988, ARA&A, 26, 631
- Bahcall, N. A., & Cen, R. 1993, ApJ, 407, L49
- Bahcall, N. A., et al. 2002, ApJ, 585, 182
- Benson, A. J., Cole, S., Frenk, C. S., Baugh, C. M., & Lacey, C. G. 2000, MNRAS, 311, 793

- Biviano, A., Girardi, M., Giuricin, G., Mardirossian, F., & Mezzetti, M. 1993, ApJ, 411, 13
- Blanchard, A., Sadat, R., Bartlett, J. G., & Le Dour, M. 2000, A&A, 362, 809
- Borgani, S., Girardi, M., Carlberg, R. G., Yee, H. K. C., & Ellington, E. 1999, ApJ, 527, 561
- Carlberg R. G., Yee H. K. C., Morris S. L., Lin H., Hall P. B., Patton D. R., Sawicki M. & Shepherd C. W. 2001, ApJ, 552, 427
- Crone, M. M., & Geller, M. J. 1995, AJ, 110, 21
- Danese, L., De Zotti, C., & di Tullio, G. 1980, A&A, 82, 322
- Diaferio, A., Ramella, M., Geller, M. J., & Ferrari, A. 1993, AJ, 105, 2035
- Diaferio, A., Kauffmann, G., Colberg, J. M, & White, S. D. M. 1999 MNRAS, 307, 537
- Edge, A. C., Stewart, G. C., Fabian, A., & Arnaud, K. A. 1990, MNRAS, 245, 559
- Fadda, D., Girardi, M., Giuricin, G., Mardirossian, F., & Mezzetti, M. 1996, ApJ, 473, 670
- Falco, E. E., et al. 1999, PASP, 111, 438 (UZC)
- Frenk, C. S., White, S. D. M., Efstathiou, G., & Davis, M. 1990, ApJ, 351, 10
- Gal, R. R., de Carvalho, R. R., Lopes, P. A. A., Djorgovski, S. G., Brunner, R. J., Mahabal, A., & Odewahn, S.C. 2003, AJ, in press
- Girardi, M., Borgani, S., Giuricin, G., Mardirossian, F., & Mezzetti, M. 1998, ApJ, 506, 45
- Girardi, M. & Giuricin, G. 2000, ApJ, 540, 45
- Girardi, M., Manzato, P., Mezzetti, M., Giuricin, G., & Limboz, F. 2002, ApJ, 569, 720
- Giuricin, G., Marinoni, C., Ceriani, L., and Pisani, A. 2000, ApJ, 543, 178
- Governato, F., Babul, A., Quinn, T., Tozzi, P., Baugh, C. M., Katz, N., & Lake, G. 1999, MNRAS, 307, 949
- Heinämäki, P., Einasto, J., Einasto, M., Saar, E., Tucker, D. L. & Müller, V. 2003, A&A, 397, 63
- Henry, J. P. 2000, ApJ, 534, 565
- Henry, J. P., & Arnaud, K. A. 1991, ApJ, 372, 410

- Huchra, J. P., & Geller, M. J. 1982, ApJ, 257, 423
- Ikebe, Y., Reiprich, T. H., Böhringer, H., Tanaka, Y., & Kitayama, T. 2002, A&A, 383, 773
- Jenkins, A., Frenk, C. S., White, S. D. M., Colberg, J. M., Cole S., Evrard A. E., Couchman H. M. P. & Yoshida N. 2001, MNRAS, 321, 372
- Kauffmann, G., Colberg, J. M., Diaferio, A. & White, S. D. M. 1999, MNRAS, 303, 188
- Lacey, C., & Cole, S. 1994, MNRAS, 271, 676
- Ledermann W. 1984 Handbook of Applicable Mathematics (Wiley and Sons), Vol. VI part A
- Lumsden, S. L., Nichol, R. C., Collins, C. A., & Guzzo, L. 1992, MNRAS, 258, 1 (EDCC)
- Mahdavi, A. 1999, private communication
- Mahdavi, A., Geller, M. J., Böhringer, H., Kurtz, M. J., & Ramella, M. 1999, ApJ, 518, 69
- Mahdavi, A. Böhringer, H., Geller, M. J., & Ramella, M. 2000, ApJ, 534, 114
- Mahdavi, A., & Geller, M. J. 2001, ApJ, 554, 129
- Mahdavi, A. 1999, private communication
- Markevitch, M. 1998, ApJ, 504, 27
- Marzke, R. O., Geller, M. J., Huchra, J. P., & Corwin, H. G. Jr., 1994, AJ, 108, 437
- Mazure, A., et al. 1996, A&A, 310, 31
- Martínez, H. J., Zandivarez, A., Merchán, M. E., & Domínguez, M. J. L. 2002, MNRAS, 337, 1441
- Materne, J. 1979, å, 74, 235
- Merchán, M. E., & Zandivarez, A. 2002, MNRAS, 335, 216
- Moore, B., Frenk, C. S. & White, S. D. M. 1993, MNRAS, 261, 827
- Nolthenius, R., Klypin, A., & Primack, J. R. 1994, ApJ, 422, L45
- Padmanabhan, N., Tegmark, M., & Hamilton, A. J. S. 2001, ApJ, 550, 52
- Pierpaoli, E., Scott, D., & White, M. 2001, MNRAS, 325, 77

- Press, W. H. & Schechter, P. 1974, ApJ, 187, 425
- Ramella M., Geller M. J. & Huchra, J. P. 1989, ApJ, 344, 57
- Ramella, M., Geller, M. J., Huchra, J. P. 1995, & Thorstensen, J. R. AJ, 109, 1469
- Ramella, M., Focardi, P., & Geller, M. J. 1996, A&A, 312, 745
- Ramella, M., Pisani, A. & Geller, M. J. 1997, AJ, 113, 483
- Ramella, M., et al. 1999, A&A, 342, 1
- Ramella, M., Geller, M. J., Pisani, A. 2002, & da Costa, L. N. AJ, 123, 2976
- Sato, S., Akimoto, F., Furuzawa, A., Tawara, Y., Watanabe, M., & Kumai, Y. 2000, ApJ, 537, 73
- Schechter, P. 1976, ApJ, 203, 297
- Reiprich T. H., & Böhringer H. 2002, ApJ, 567, 716
- Thomas, P. A., et al. 1998, MNRAS, 296, 1061
- Tucker D. L., et al. 2000, ApJS, 130, 237
- Tully, R. B. 1987, ApJ, 321, 280
- Turner, E. L. & Gott, J. R., III 1976, ApJS, 32, 409
- Trasarti-Battistoni, R. 1998, A&AS, 130, 341
- Valageas, P., & Schaeffer, R. 1997, A&A, 328, 435
- Weinberg, D. H. & Cole, S. 1993, MNRAS, 259, 652
- Xu, W., Fang, L, & Wu, X. 2000, ApJ, 532, 728
- Yee, H. K. C. & Ellingson, E. 2003, ApJ, 585, 215
- Zabludoff A., Geller M. J., Huchra, J. P., & Ramella, M. 1993, AJ, 106, 1301
- Zabludoff, A., & Geller, M., J. 1994, AJ, 107, 1929
- Zandivarez, A., Abadi, M. G., & Lambas, D. G. 2001, MNRAS, 326, 147

This preprint was prepared with the AAS IAT_EX macros v5.0.

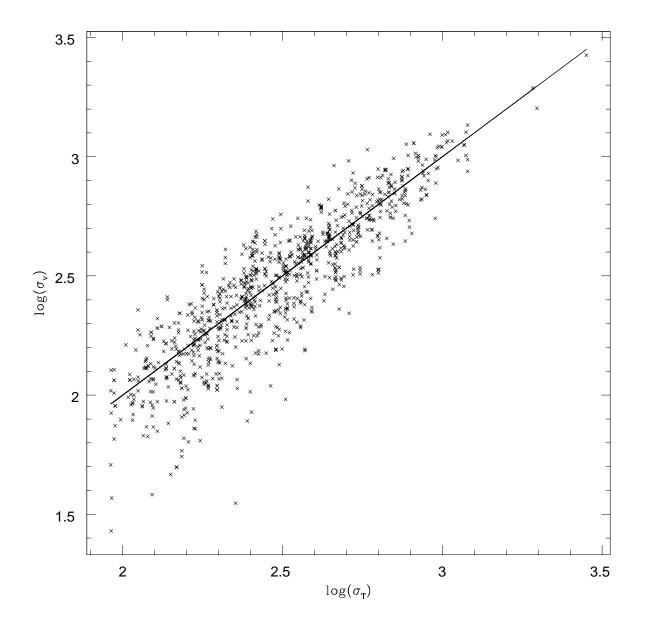


Fig. 1.— The relation between the true velocity dispersion σ_T and observed velocity dispersion σ_v for a Monte Carlo simulation. The solid line represents the identity.

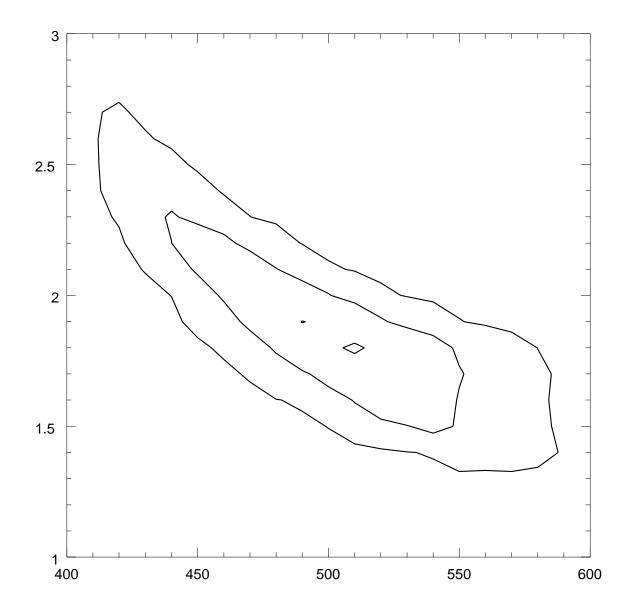


Fig. 2a.— The contour levels of the model N versus σ_T (eq. 1) for the UZCGG groups with 5 or more members. The outer thick contour traces the 99% confidence region, the middle contour traces the 90% confidence level, and the inner thin contour traces the 50% confidence level.

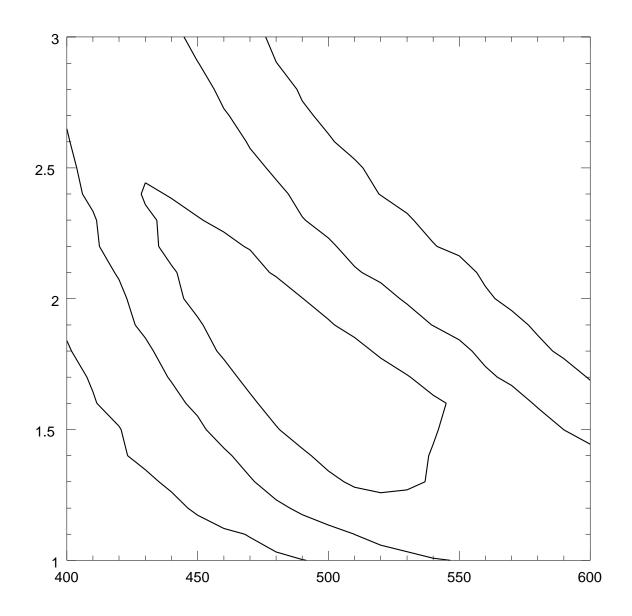


Fig. 2b.— Same as Figure 2a for x-ray emitting groups

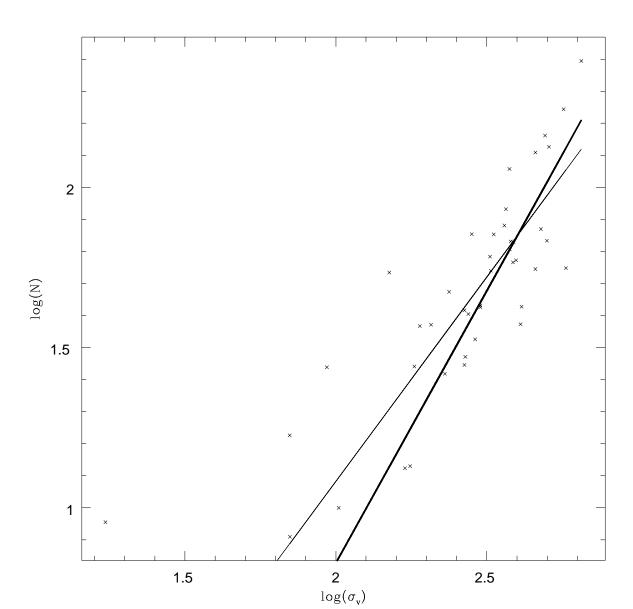


Fig. 3.— The relation between the group richness N and the velocity dispersion σ_v for the x-ray emitting groups. The thin line results from the bisector of the two least squares straight lines (one by fitting N vs. σ_v and the other by fitting σ_v vs. N), the thick line shows that our Monte Carlo approach has less sensitivity to low σ_v groups.

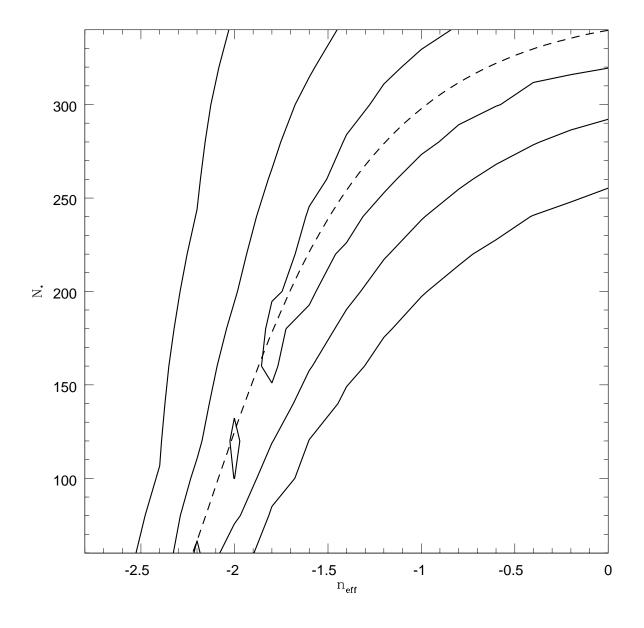


Fig. 4.— The PS model: the contours show the KS test significance level $S_{KS}(N_{mem})$ for the comparison between the observed distribution of the groups and the PS model described by N_{\star} and the effective spectral index n_{eff} . The outer contours indicate the 99% confidence level, the middle contours indicate the 50% confidence level and the inner contours show the 10% confidence level. The dot-dashed line shows the relation for data distributed according to a power law (eq. 10) and with $\langle N \rangle = 300$, $\gamma = 2.9$ and k = 1.43. The power-law line lies well within the 50% confidence level. The relation between the group richness N and mass is $M \propto N^{1.43}$ (see Table 1).

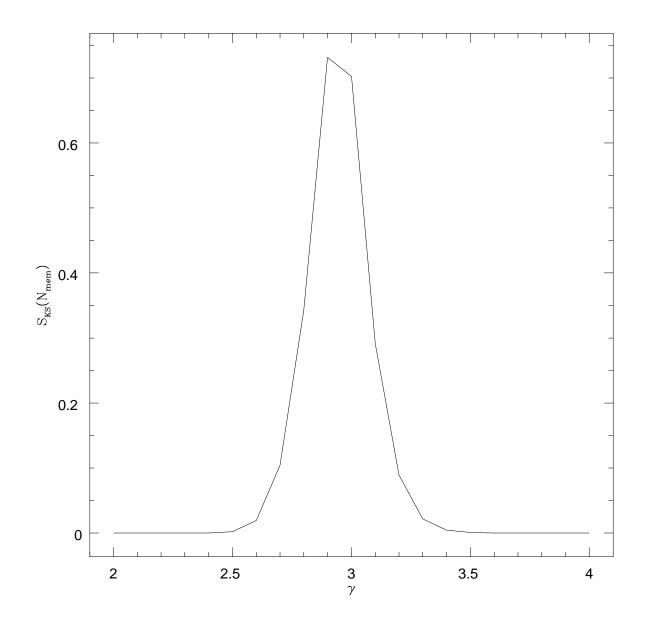


Fig. 5.— The power law model: the KS test significance level $S_{KS}(N_{mem})$ for the comparison between the model and observed distribution of the group members.

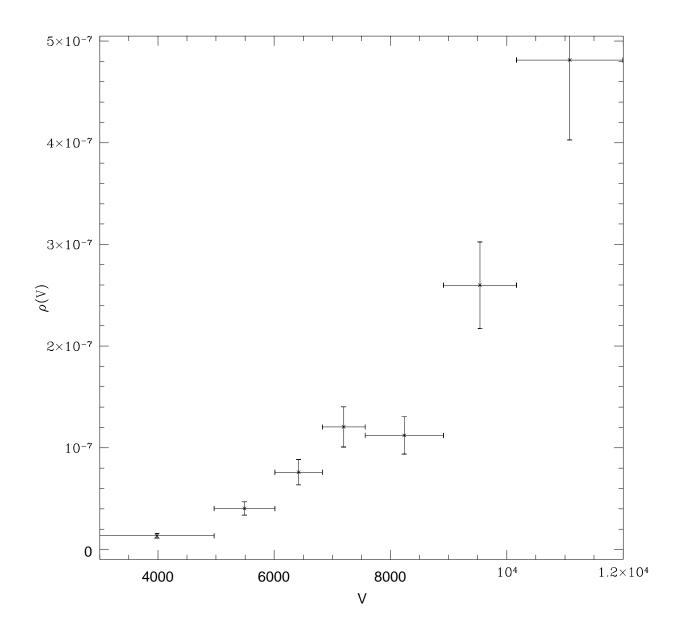


Fig. 6.— [Fig. 6] The density of groups as a function of the radial distance $\rho(V)$. The function is the best fit power law model for p(N) with $N_{shell} = 7$ intervals. The error bars in V are the width of the bins; for ρ they the Poisson uncertainty δN_i in the number of groups per bin.

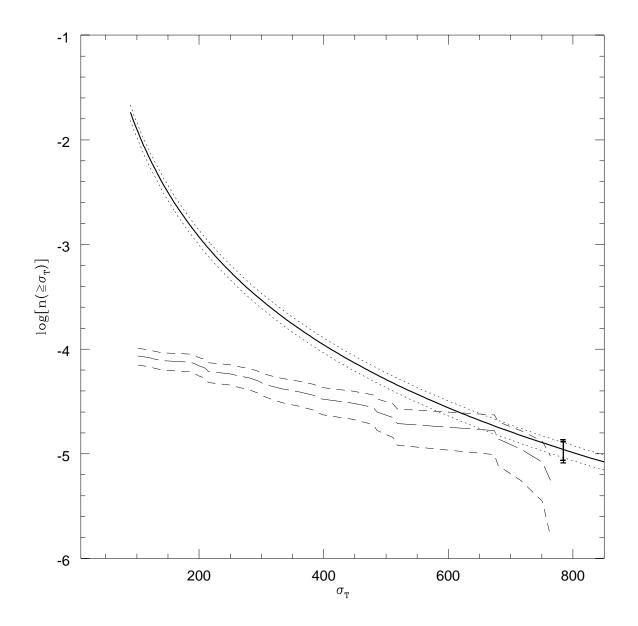


Fig. 7.— The power law model for the space density of groups with true velocity dispersion $\geq \sigma_T$. The thin curve shows the power law model (Eq. 23), the dotted lines show the 95% confidence band for the entire range of σ_T . The right side vertical bar shows the width of the 95% confidence level for the observed density of robust groups. The dashed curves show the data of Zabludoff et al. (1993) ($\pm 1 - \sigma$ poissonian error band).

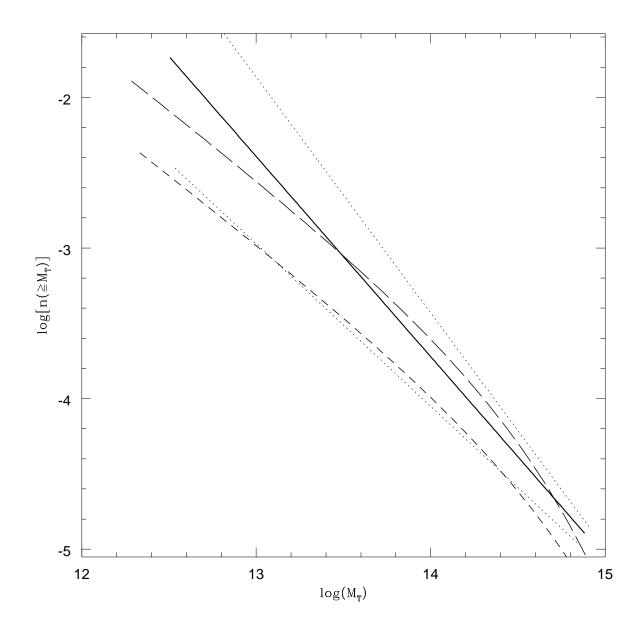


Fig. 8.— The cumulative mass function of groups (thick solid line). Dotted lines are 95% confidence levels. The thick short- and long-dashed lines are theoretical predictions (Jenkins et al. 2001) for Λ CDM ($\Omega_m = 0.3, \Omega_{\Lambda} = 0.7, \sigma_8 = 0.9$) and τ CDM with ($\Omega_m = 1, \Omega_{\Lambda} = 0, \sigma_8 = 0.6$) models respectively.

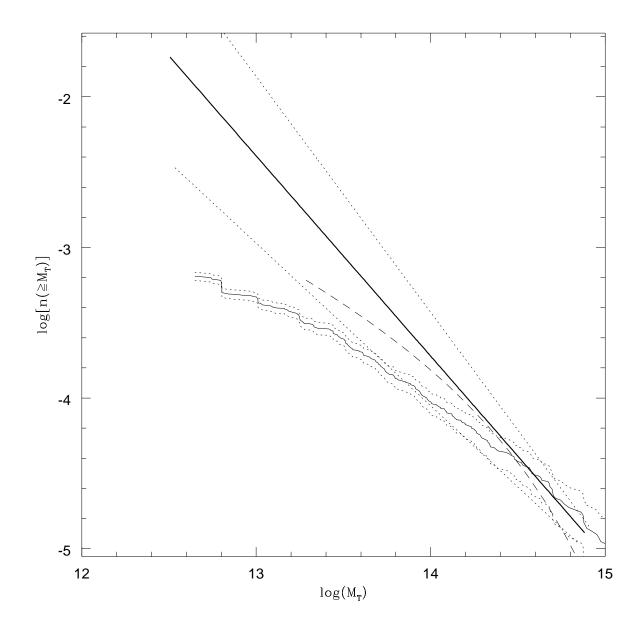


Fig. 9.— The cumulative mass function of groups (thick solid line). Dotted lines are 95% confidence levels. The dashed line shows the results obtained by Girardi & Giuricin (2000). The thin solid curve is the observed mass function we obtain assuming constant large scale density of groups.

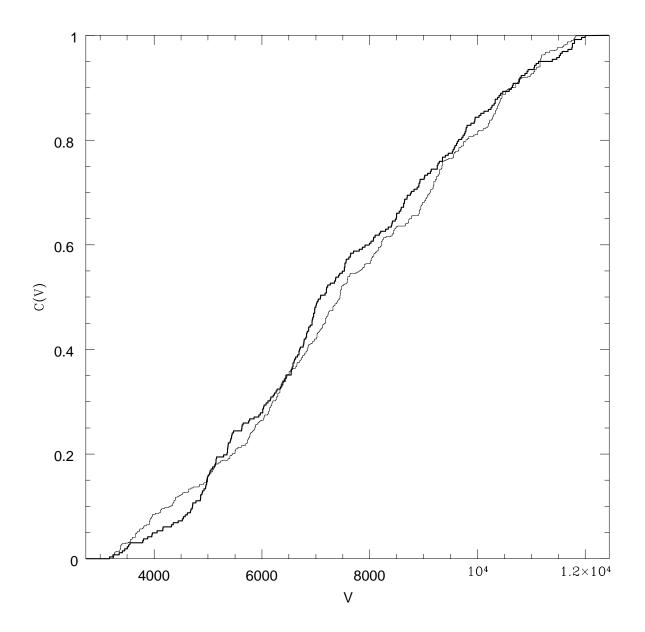


Fig. 10a.— [Figure 10a] The Power Law model for the group pdf: the observed and model cumulative distribution of radial velocity V of UZCGG groups (thick curve) and a 1000 group Monte Carlo simulation of our best fit power law model (thin curve).

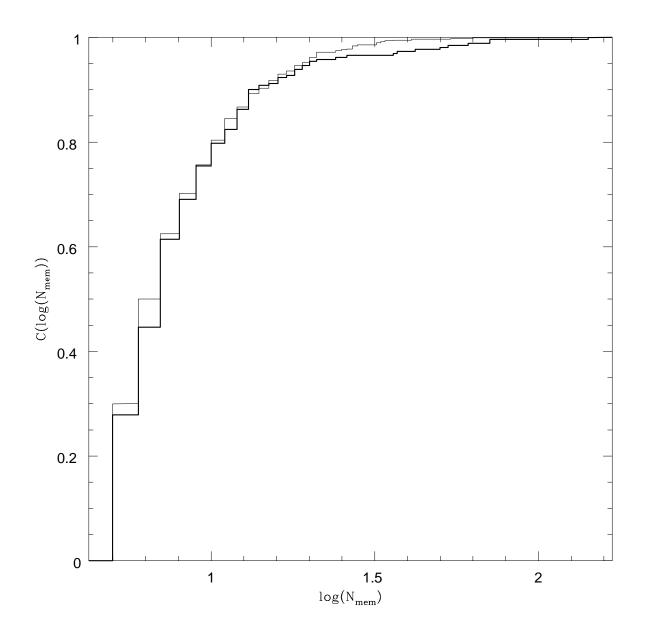


Fig. 10b.— [Figure 10b] The power law model for the group pdf: observed and model cumulative distribution of N_{mem} of UZCGG groups (thick curve) and a 1000 group Monte Carlo simulation of our best fit power law model (thin curve).]

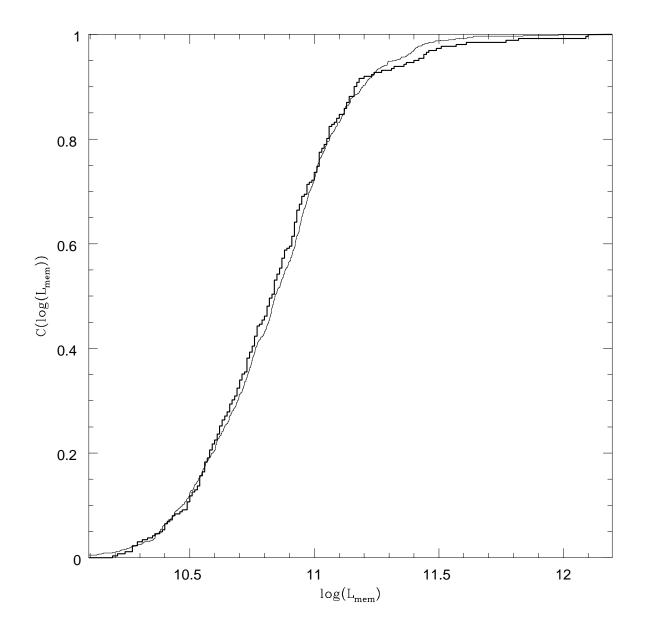


Fig. 10c.— [Figure 10c] The power law model for the group pdf: observed and model cumulative distribution of $\log(L_{mem})$ of UZCGG groups (thick curve) and a 1000 group Monte Carlo simulation of our best fit power law model (thin curve).]

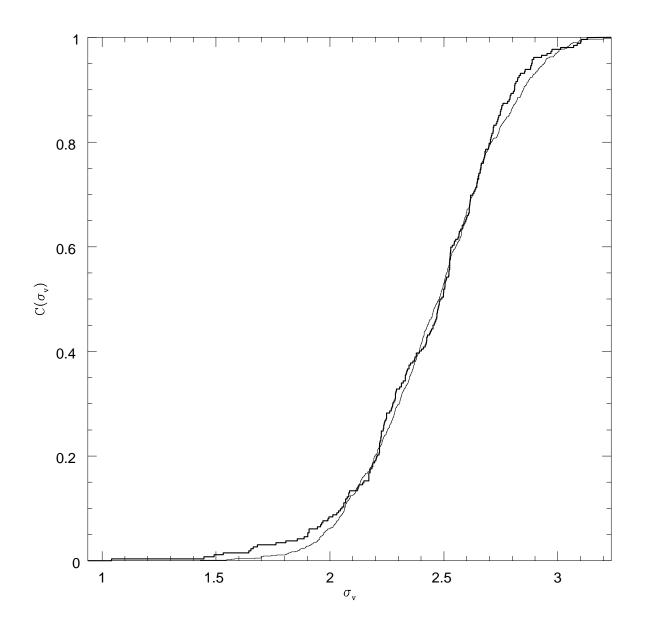


Fig. 10d.— [Figure 10d] The power law model for the group pdf: observed and model cumulative distribution of σ_v of UZCGG groups (thick curve) and a 1000 group Monte Carlo simulation of our best fit power law model (thin curve).]

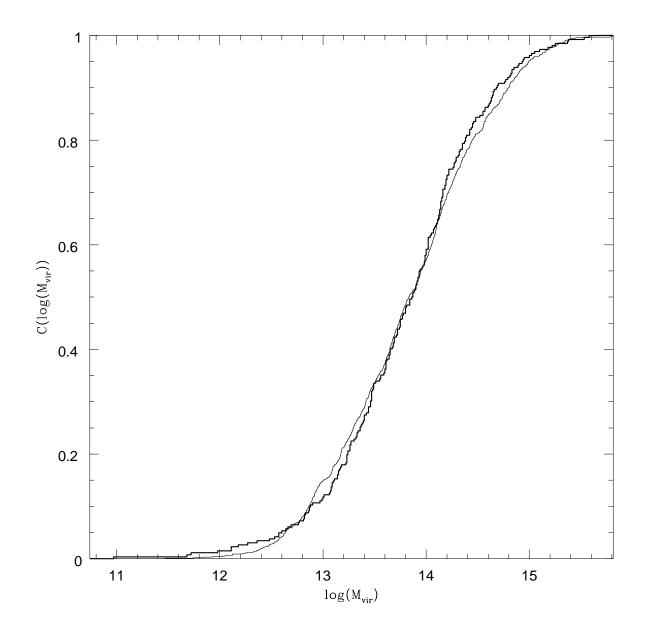


Fig. 10e.— [Figure 10e] The power law model for the group pdf: observed and model cumulative distribution of virial mass M_{vir} of UZCGG groups (thick curve) and a 1000 group Monte Carlo simulation of our best fit power law model (thin curve).]

Table 1. The scaling relations among the main group parameters.

Relation	Slope	Intercept
$log(M_T) \text{ vs. } log(N)$ $log(M_T) \text{ vs. } log(L_T)$ $log(M_T) \text{ vs. } log(\sigma_T)$ $log(L_T) \text{ vs. } log(\sigma_T)$ $log(N) \text{ vs. } log(R_{vir})$ $log(\sigma_T) \text{ vs. } log(R_{vir})$	$\begin{array}{c} 1.43\substack{+0.04\\-0.04}\\ 1.44\substack{+0.06\\-0.06}\\ 2.58\substack{+0.07\\-0.07}\\ 1.80\substack{+0.05\\-0.04}\\ 2.00\substack{+1.54\\-0.88}\\ 1.18\substack{+0.88\\-0.45}\end{array}$	$\begin{array}{c} 10.70^{+0.08}_{-0.09} \\ -2.21^{+0.66}_{-0.71} \\ 7.48^{+0.16}_{-0.18} \\ 6.71^{+0.11}_{-0.11} \\ 2.11^{+0.06}_{-0.02} \\ 2.42^{+0.03}_{-0.08} \end{array}$